Inorg. Chem. **2003**, *42*, 7319–7325

$MA_\delta Sb_{2-\delta}$ (M = Zr, Hf; A = Si, Ge): A New Series of Ternary Antimonides and Not "β-$ZrSb_2$"

Navid Soheilnia, Abdeljalil Assoud, and Holger Kleinke*

Department of Chemistry, University of Waterloo, Waterloo, Ontario, Canada N2L 3G1

Received June 30, 2003

The ternary antimonides $ZrSi_\delta Sb_{2-\delta}$, $HfGe_\delta Sb_{2-\delta}$, and $ZrGe_\delta Sb_{2-\delta}$ were prepared by annealing of the elements in stoichiometric ratios below 800 °C. $ZrSi_\delta Sb_{2-\delta}$ was earlier erroneously described as the binary "β-$ZrSb_2$", which does not exist as such, because the incorporation of tetrel atoms is necessary for the formation of this structure. $ZrSi_\delta Sb_{2-\delta}$ has a small yet significant phase width with at least $0.066(7) \le \delta \le 0.115(3)$, whereas the Ge analogues exist with larger tetrel concentration, i.e., $ZrGe_{0.211(5)}Sb_{1.789}$ and $HfGe_{0.205(6)}Sb_{1.795}$. The whole series of title compounds crystallizes in the Co_2Si type (space group *Pnma*), with lattice dimensions of, e.g., for $ZrGe_{0.211(5)}Sb_{1.789}$, a = 730.4(1) pm, b = 395.13(6) pm, c = 957.6(2) pm, V = 0.27635(7) nm^3, Z = 4. The anionic substructure comprises infinite ribbons formed by the atom sites Q1 and Sb2, with Q1 being mixed occupied by Si or Ge and Sb atoms. These ribbons exhibit Q1–Q1 single bonds and Q1–Sb2 "half" bonds. Assuming the validity of the 8 – N rule, one can assign seven valence-electrons to Sb2 but only five to Q1, which might explain the preference of the tetrel atoms for the latter site.

Introduction

The discovery of the outstanding thermoelectric properties of the filled skutterudites LnM_4Sb_{12} (Ln = lanthanoid, M = Fe, Co, Ni, ...) sparked an enormous amount of research into this structure family. E.g., $LaFe_3CoSb_{12}$, a small-gap semiconductor, exhibits a moderate Seebeck coefficient, a relatively good electrical conductivity, and a very low thermal conductivity. The latter is a consequence of the rattling of the Ln atom situated in a large icosahedral void of the three-dimensional Sb atom network. The combination of these properties results in an unprecedented figure-of-merit of 1.4 (at 730 °C).[1–9]

As thermoelectric materials are usually narrow-gap semiconductors (i.e. comprising a gap < 0.6 eV), this electronic fingerprint is evidently necessary for the thermoelectric energy conversion.[10] Our research group carries out exploratory synthesis of early transition metal antimonides and chalcogenides with the long-term goal of discovering comparable Sb/Te atom substructures in semiconducting materials. To date, we found new, the first Sb-based, representatives of the Nowotny chimney ladder phases,[11–13] namely $(Ti,M)_5Sb_8$ (M = Ti, Zr, Hf, Nb)[14,15] and $(Zr,V)_{11}Sb_{18}$.[16] The rattling effect was evident in $Zr_2V_6Sb_9$.[17] None of these antimonides exhibited semiconducting properties, however. These were identified in $Mo_3Sb_5Te_2$,[18] which forms a structure containing empty Sb_8 cubes. We subsequently

* To whom correspondence should be addressed. E-mail: kleinke@uwaterloo.ca. Fax: +1 (519) 746-0435.

(1) Sales, B. C.; Mandrus, D.; Williams, R. K. *Science (Washington, D.C.)* **1996**, *272*, 1325−1328.
(2) Katsuyama, S.; Shichijo, Y.; Ito, M.; Majima, K.; Nagai, H. *J. Appl. Phys.* **1998**, *84*, 6708−6712.
(3) Fornari, M.; Singh, D. J. *Phys. Rev. B* **1999**, *59*, 9722−9724.
(4) Nolas, G. S.; Morelli, D. T.; Tritt, T. M. *Annu. Rev. Mater. Sci.* **1999**, *29*, 89−116.
(5) Dilley, N. R.; Bauer, E. D.; Maple, M. B.; Dordevic, S.; Basov, D. N.; Freibert, F.; Darling, T. W.; Migliori, A.; Chakoumakos, B. C.; Sales, B. C. *Phys. Rev. B* **2000**, *61*, 4608−4614.
(6) Kitagawa, H.; Hasaka, M.; Morimura, T.; Nakashima, H.; Kondo, S. I. *Mater. Res. Bull.* **2000**, *35*, 185−192.
(7) Takizawa, H.; Ito, M.; Uheda, K.; Endo, T. *J. Ceram. Soc. Jpn.* **2000**, *108*, 530−534.
(8) Dilley, N. R.; Bauer, E. D.; Maple, M. B.; Sales, B. C. *J. Appl. Phys.* **2000**, *88*, 1948−1951.
(9) Dyck, J. S.; Chen, W.; Uher, C.; Chen, L.; Tang, X.; Hirai, T. *J. Appl. Phys.* **2002**, *91*, 3698−3705.
(10) Rowe, D. M. *CRC Handbook of Thermoelectrics*; CRC Press: Boca Raton, FL, 1995.
(11) Flieher, G.; Völlenkle, H.; Nowotny, H. *Monatsh. Chem.* **1968**, *99*, 2408−2415.
(12) Pearson, W. B. *Acta Crystallogr. B* **1970**, *26*, 1044−1046.
(13) Lu, G.; Lee, S.; Lin, J.; You, L.; Sun, J.; Schmidt, J. T. *J. Solid State Chem.* **2002**, *164*, 210−219.
(14) Kleinke, H. *Inorg. Chem.* **2001**, *40*, 95−100.
(15) Zhu, Y.; Kleinke, H. *Z. Anorg. Allg. Chem.* **2002**, *628*, 2233.
(16) Elder, I.; Lee, C.-S.; Kleinke, H. *Inorg. Chem.* **2002**, *41*, 538−545.
(17) Kleinke, H. *Eur. J. Inorg. Chem.* **1998**, 1369−1375.
(18) Dashjav, E.; Szczepenowska, A.; Kleinke, H. *J. Mater. Chem.* **2002**, *12*, 345−349.

10.1021/ic0347440 CCC: $25.00
Published on Web 10/02/2003

succeeded in partly filling these cubes in attempts to create the rattling effect.[19]

We prepared $ZrSb_2$[20] as a starting material for the synthesis of several of these compounds and others.[21−23] We always produced the so-called α-form and never found the "β-modification", which was described to exist as slightly Sb-deficient on one of the two Sb sites.[24] Both forms are of special theoretical interest because of their nonclassical bonding within the different Sb atom substructures.[25] Recently, we encountered the "β-modification" in an attempt to produce large single crystals of $ZrSb_2$ by using iodine as chemical transport agent. Subsequently our investigations proved that "β-$ZrSb_2$" does not exist as written; rather it is a ternary zirconium silicide antimonide ($ZrSi_\delta Sb_{2-\delta}$) crystallizing in the TiNiSi type. We succeeded in preparing its isostructural variants $ZrGe_\delta Sb_{2-\delta}$ and $HfGe_\delta Sb_{2-\delta}$ as well, while the Sn-containing antimonide was described elsewhere.[26]

Experimental Section

Synthesis. We found $ZrSi_\delta Sb_{2-\delta}$ as the unintended main product of a reaction of 2 mmol of elemental zirconium and 4 mmol of elemental antimony and traces (<10 mg) of elemental iodine. All elements were used as acquired from Aldrich and Alfa Aesar, with nominal purities of at least 98.5%. The reaction mixture was put into a fused silica tube, which was then sealed under vacuum to prevent the formation of oxides. The fused silica tube was annealed at 700 °C in a resistance furnace over a period of 1 week. Tube attack, i.e., a reaction of the sample with the reaction container comprising silicon and oxygen, was evident, as the tube was obfuscated at the bottom where the sample was located. The reaction mixture itself appeared to be metallic, grayish microcrystalline powder with some large bar-shaped crystals of metallic luster.

The X-ray powder diffractogram of this mixture (INEL powder diffractometer with position sensitive detector) consisted almost exclusively of the reflections of so-called "β-$ZrSb_2$". Since Si and/or O incorporation was suspected, we carried out EDAX investigations (LEO 1530, with integrated EDAX Pegasus 1200) on selected crystals, which revealed the presence of Zr, Si, and Sb in the ratio of 33:5:62 (in at-%). The subsequent single-crystal structure study resulted in a refined formula of $ZrSi_{0.066(7)}Sb_{1.934}$ (at. %: 33.3:2.2:64.5) in the TiNiSi structure, an ordered variant of Co_2Si (for details see below).

To address the questions whether the incorporation of silicon is essential for the formation of this structure and whether oxygen and iodine need to be present, a series of reactions was carried out with purposefully adding silicon but neither oxygen nor iodine. Control reactions were carried out starting from Zr and Sb, without adding any heteroelements. We also investigated the use of different reaction containers, i.e., ceramic crucibles (Al_2O_3-based), and replaced silicon with germanium. The reaction temperatures were chosen to range from 650 to 1000 °C.

We identified the target structure (TiNiSi type, so-called "β-$ZrSb_2$") in all reactions with silicon and germanium, independent of the temperature and the reaction container. Neither oxygen nor iodine was required for its formation. Since it never occurred without the presence of silicon or germanium, we conclude that it cannot exist without the incorporation of a tetrel.

To study a possible phase range of $ZrSi_\delta Sb_{2-\delta}$, we carried out a small set of reactions with different Si:Sb ratios at 700 °C (reactions 1−3). We checked for the existence of isostructural compounds with the reactions 4−7 and identified the following main products on the basis of their X-ray powder diffractograms:

$$Zr + 0.1Si + 1.9Sb \rightarrow ZrSi_\delta Sb_{2-\delta} \quad (1)$$

$$Zr + 0.2Si + 1.8Sb \rightarrow ZrSi_\delta Sb_{2-\delta} + ZrSi_{0.7}Sb_{1.3} \quad (2)$$

$$Zr + 0.3Si + 1.7Sb \rightarrow ZrSi_\delta Sb_{2-\delta} + ZrSi_{0.7}Sb_{1.3} \quad (3)$$

$$Ti + 0.1Si + 1.9Sb \rightarrow TiSb_2 + Si \quad (4)$$

$$Hf + 0.1Si + 1.9Sb \rightarrow HfSb_2 + Si \quad (5)$$

$$Zr + 0.2Ge + 1.8Sb \rightarrow ZrGe_\delta Sb_{2-\delta} \quad (6)$$

$$Hf + 0.2Ge + 1.8Sb \rightarrow HfGe_\delta Sb_{2-\delta} \quad (7)$$

$ZrSi_{0.7}Sb_{1.3}$[26] crystallizes in the ZrSiS type with square nets of Si atoms. We conclude on the basis of the reactions 2 and 3 that the Si content of $ZrSi_\delta Sb_{2-\delta}$ (TiNiSi type) cannot reach $\delta = 0.2$. The attempts to replace Zr with Hf and Ti in the Si-containing system did not lead to the formation of the TiNiSi type. On the other hand, the two reactions 6 and 7 resulted in virtually phase pure samples of the TiNiSi type, pointing toward a larger phase range of both $ZrGe_\delta Sb_{2-\delta}$ and $HfGe_\delta Sb_{2-\delta}$ compared to $ZrSi_\delta Sb_{2-\delta}$.

Single-Crystal Structure Studies. All single-crystal structure studies were performed with the Smart APEX CCD diffractometer from Bruker. Data were collected by scans of 0.3° in ω in groups of 606 frames. Data reduction and refinement were done using the SAINT[27] and SHELXTL[28] packages. The 2θ values varied between 3 and 70°. The data were corrected for Lorentz and polarization effects. Absorption corrections were based on fitting a function to the empirical transmission surface as sampled by multiple equivalent measurements. Diffraction peaks obtained from all frames of reciprocal space images were used to determine the unit cell parameters. Four different single crystals were studied, the first one coming from the transport reaction of Zr and Sb and the other three from the reactions 3, 6, and 7. In all four case studies, the systematic extinctions were consistent with the space group *Pnma* (and its noncentrosymmetric subgroup $Pn2_1a$), which is the space group of the TiNiSi type.

The refinements were started from the atomic positions published for the "β-$ZrSb_2$" structure, allowing for mixed Si/Sb and Ge/Sb occupancies, respectively, on both Sb sites. In each case, the refinements converged smoothly to satisfying residual values, confirming the validity of this structure model. Only one Sb site showed incorporation of the tetrel atoms, namely Sb1. We therefore label this site more correctly Q1, to indicate its mixed occupancy of Sb and tetrel atoms A. This is the site that was originally refined as being Sb-deficient, resulting in an occupancy of 95.6(4)% Sb. As expected on the basis of the powder diffractograms, the refined

(19) Soheilnia, N.; Dashjav, E.; Kleinke, H. *Can. J. Chem.*, in press.
(20) Kjekshus, A. *Acta Chem. Scand.* **1972**, *26*, 1633−1639.
(21) Kleinke, H. *Chem. Commun.* (*Cambridge*) **1998**, 2219−2220.
(22) Kleinke, H.; Harbrecht, B. *Z. Anorg. Allg. Chem.* **1999**, *625*, 1873−1877.
(23) Kleinke, H. *J. Am. Chem. Soc.* **2000**, *122*, 853−860.
(24) Garcia, E.; Corbett, J. D. *J. Solid State Chem.* **1988**, *73*, 452−467.
(25) Papoian, G.; Hoffmann, R. *J. Am. Chem. Soc.* **2001**, *123*, 6600−6608.
(26) Lam, R.; Mar, A. *J. Solid State Chem.* **1997**, *134*, 388−394.
(27) *SAINT*, version 4 ed.; Siemens Analytical X-ray Instruments Inc.: Madison, WI, 1995.
(28) Sheldrick, G. M. *SHELXTL Reference Manual*, version 5.12 ed.; Siemens Analytical X-ray Systems, Inc.: Madison, WI, 1995, 1996.

Table 1. Crystallographic Data for $MA_\delta Sb_{2-\delta}$[a]

param	chem formula			
	$ZrSi_{0.07}Sb_{1.93}$	$ZrSi_{0.12}Sb_{1.88}$	$ZrGe_{0.21}Sb_{1.79}$	$HfGe_{0.20}Sb_{1.80}$
fw	328.63	323.95	322.97	411.91
ρ_{calcd} (g/cm^3)	7.692	7.681	7.763	10.002
a (pm)	740.1(2)	736.5(1)	730.4(1)	731.2(3)
b (pm)	398.98(9)	397.33(8)	395.13(6)	394.3(2)
c (pm)	961.0(2)	957.4(2)	957.6(2)	948.8(4)
V (nm^3)	0.2838(1)	0.28014(1)	0.27635(7)	0.2735(2)
μ (cm^{-1})	215.67	213.96	230.02	573.14
$R(F_o)^b/R_w(F_o^2)^c$	0.043/0.097	0.026/0.056	0.049/0.083	0.042/0.067

[a] M = Zr, Hf; A = Si, Ge; *T* of measurement, 298 K; λ = 71.073 pm; space group, *Pnma*; *Z* = 4. For comparison, the lattice dimensions of isostructural "β-$ZrSb_2$" are *a* = 739.3(1) pm, *b* = 398.70(7) pm, *c* = 958.1(1) pm, and *V* = 0.28242(7) nm^3. [b] $R(F_o) = \Sigma||F_o| - |F_c||/\Sigma|F_o|$. [c] $R_w(F_o^2) = [\Sigma[w(F_o^2 - F_c^2)^2]/\Sigma[w(F_o^2)^2]]^{1/2}$.

Table 2. Positional Parameters and Equivalent Displacement Parameters for $ZrGe_{0.21}Sb_{1.79}$

atom	site	x	y	z	U_{eq} (Å^2)
Zr	4c	0.2605(2)	1/4	0.1630(1)	0.0067(3)
Q1[a]	4c	0.8732(1)	1/4	0.0442(1)	0.0091(3)
Sb2	4c	0.9281(1)	1/4	0.64544(9)	0.0083(2)

[a] Occupancy: 21.1(5)% Ge, 78.9% Sb.

formulas were (almost) identical with the starting ratios of the elements in the Ge-containing cases (1:0.2:1.8), namely $ZrGe_{0.211(5)}Sb_{1.789}$ and $HfGe_{0.205(6)}Sb_{1.795}$. The two refinements in the Zr/Si/Sb system yielded refined formulas of $ZrSi_{0.066(7)}Sb_{1.934}$ and $ZrSi_{0.115(3)}Sb_{1.885}$, indicating that the latter represents the maximal possible Si content under the preparative conditions used.

Details of the four data collections are given in Table 1. Positional parameters of $ZrGe_{0.21}Sb_{1.79}$ may be found in Table 2. More details are given in the CIF file (see Supporting Information). It is noted that the lattice dimensions shrink with increasing Si content and that the data from the original publication on "β-$ZrSb_2$"[24] are between those of $ZrSi_{0.066(7)}Sb_{1.934}$ and $ZrSi_{0.115(3)}Sb_{1.885}$. It is thus likely that the Si content was between 6.6 and 11.5% on the Q1 site in that investigation.

Band Structure Calculations. Self-consistent tight-binding LMTO calculations (LMTO = linear muffin tin orbitals)[29,30] were carried out on different structure models. Therein, the density functional theory is used with the local density approximation (LDA).[31] The refined structure of $ZrGe_{0.21}Sb_{1.79}$ was chosen as basis for the structure models. For the first one, all structural parameters were retained, except for the Q1 site that was treated as a pure Sb position—modeling "β-$ZrSb_2$". To visualize the changes that might occur upon Ge incorporation, we lowered the symmetry to *Pm* to obtain four independent positions of the Q1 site. One thereof was assigned a Ge atom, while the other three remained Sb. This models the formula "$ZrGe_{0.25}Sb_{1.75}$". The integration in *k* space was performed by an improved tetrahedron method[32] on grids of sufficient independent *k* points of the first Brillouin zone, namely 624 and 1560, respectively. All cases were checked for *k* point consistency.

Physical Property Measurements. The product of the reaction 6, identified as $ZrGe_{0.2}Sb_{1.8}$, was chosen for the physical property determinations. Seebeck coefficients *S* were determined on a bar of the dimensions of 5 × 1 × 1 mm, cold-pressed using a force of 10 kN. A commercial thermopower measurement apparatus (MMR Technologies) was used to measure *S* under dynamic vacuum in the temperature range between 300 and 600 K, using constantan as an internal standard to determine the temperature difference. Silver paint (AMI DODUCO Technology) was used to create the electric contacts.

Specific resistivities ρ were measured using a four-point method at the same bar that was used for the Seebeck coefficient determinations. A self-made device was used to measure the voltage drops ΔV over a distance of 3 mm at constant current of 10 mA under dynamic vacuum between 300 and 170 K, wherein cooling was achieved by helium compression.

Results and Discussion

Crystal Structure. According to our experimental data, "β-$ZrSb_2$" can only be formed with mixed A/Sb occupancies on the Q1 site (A = Si, Ge, Sn). Therefore, it is not a *binary* Zr antimonide, i.e., *not* β-*ZrSb*$_2$, but a ternary phase. As the mixed occupancies are necessary for the phase formation, and they differ between the two anionic sites ("Sb1" and Sb2), $ZrA_\delta Sb_{2-\delta}$ (and $HfGe_{0.2}Sb_{1.8}$) may be classified as anionic DFSO materials (DFSO = differential fractional site occupancies). DFSO materials are stabilized by mixed occupancies in different ratios on crystallographically independent sites, originally metal atom sites of metal-rich sulfides. This concept was introduced in the early 1990s[33,34] after the uncovery of four ternary niobium tantalum sulfides, namely $Nb_{1.72}Ta_{3.28}S_2$,[35] $Nb_{0.95}Ta_{1.05}S$,[36] $Nb_{4.92}Ta_{6.08}S_4$,[37] and $Nb_{6.74}Ta_{5.26}S_4$.[38] If one allows some metal atom sites being occupied by either of the metal atoms alone, the earliest examples of DFSO compounds were published in 1987, namely $M_\delta Ta_{6-\delta}S$ with $\delta \approx 1$ and M = V and Cr.[39] It was subsequently shown that other transition metal atom pairs may be used as well, e.g. in $Zr_{3.66}Ti_{3.34}Sb_7$ (new structure type),[23] $Hf_{5.95}Ti_{1.05}Sb_4$,[40] $Zr_{7.5}V_{5.5}Sb_{10}$ (new type),[21] $Zr_{7.46}V_{3.54}Sb_8$ ($Cr_{11}Ge_8$ type),[41] $Zr_{6.45}Nb_{4.55}P_4$ (new type),[42] $Hf_{5.08}$-

(29) Andersen, O. K. *Phys. Rev. B* **1975**, *12*, 3060−3083.
(30) Skriver, H. L. *The LMTO Method*; Springer: Berlin, 1984.
(31) Hedin, L.; Lundqvist, B. I. *J. Phys. C* **1971**, *4*, 2064−2083.
(32) Blöchl, P. E.; Jepsen, O.; Andersen, O. K. *Phys. Rev. B* **1994**, *49*, 16223−16233.
(33) Yao, X.; Marking, G.; Franzen, H. F. *Ber. Bunsen-Ges.* **1992**, *96*, 1552−1557.
(34) Köckerling, M.; Franzen, H. F. *Croat. Chem. Acta* **1995**, *68*, 709−719.
(35) Yao, X.; Franzen, H. F. *J. Am. Chem. Soc.* **1991**, *113*, 1426−1427.
(36) Yao, X.; Miller, G. J.; Franzen, H. F. *J. Alloys Compd.* **1992**, *183*, 7−17.
(37) Yao, X.; Franzen, H. F. *J. Solid State Chem.* **1990**, *86*, 88−93.
(38) Yao, X.; Franzen, H. F. *Z. Anorg. Allg. Chem.* **1991**, *598−599*, 353−362.
(39) Harbrecht, B.; Franzen, H. F. *Z. Anorg. Allg. Chem.* **1987**, *551*, 74−84.
(40) Kleinke, H. *Inorg. Chem.* **1999**, *38*, 2931−2935.
(41) Kleinke, H. *J. Mater. Chem.* **1999**, *9*, 2703−2708.
(42) Marking, G. A.; Franzen, H. F. *Chem. Mater.* **1993**, *5*, 678−680.

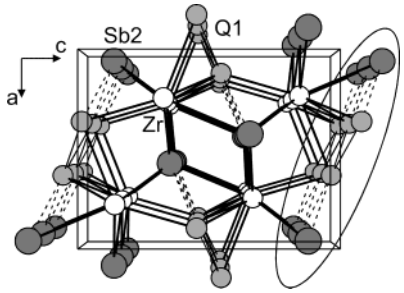

Figure 1. Crystal structure of $ZrA_\delta Sb_{2-\delta}$ in a projection along the *b* axis: white circles, Zr; medium gray, Q1 (A/Sb); large dark gray, Sb2.

Table 3. Selected Interatomic Distances (pm) for $MA_\delta Sb_{2-\delta}$

bond	no.	$ZrSi_{0.07}Sb_{1.93}$	$ZrSi_{0.12}Sb_{1.88}$	$ZrGe_{0.21}Sb_{1.79}$	$HfGe_{0.20}Sb_{1.80}$
M−Q1	1	293.1(2)	292.2(1)	292.2(2)	289.7(2)
M−Q1	2	298.4(1)	297.22(7)	296.5(1)	295.3(1)
M−Q1	1	309.3(2)	307.6(1)	304.9(2)	304.4(2)
M−Sb2	2	303.8(1)	302.74(7)	301.7(1)	300.3(1)
M−Sb2	2	306.2(1)	304.92(7)	302.7(1)	302.2(1)
M−Sb2	1	321.8(2)	320.1(1)	319.8(2)	317.9(2)
Q1−Q1	2	288.6(1)	286.70(8)	283.8(2)	283.5(2)
Q1−Sb2	2	314.9(1)	313.50(7)	311.1(1)	312.1(2)

$Mo_{0.92}P_3$ (new type),[43] $Hf_{1.06}Mo_{0.94}P$ (Fe_2P type),[44] and $Hf_{4.96}Nb_{5.04}Ni_3P_5$ (new type).[45]

Although actual examples are rather scarce,[46] the very same concept can be applied to mixing the anionic elements, e.g. Se and Te atoms, on various sites in different ratios, as shown with the uncovery of $Ta_5Se_{1.2}Te_{1.8}$[47] and $Zr_7Sb_{1.6}Se_{2.4}$.[22] Thus far, two antimonides are known with mixed Si/Sb occupancies, namely $ZrSi_{0.7}Sb_{1.3}$[26] and $Ti_5Si_{1.3}Sb_{1.7}$,[48] while $ZrGe_{0.21}Sb_{1.79}$ and $HfGe_{0.2}Sb_{1.8}$ are the first examples with mixed Ge/Sb occupancies (to our knowledge).

The structure type of the title compounds, Co_2Si—or, more precisely, TiNiSi— has many representatives. The ones most similar to $ZrA_\delta Sb_{2-\delta}$ are ZrP_2[49] and $ZrAs_2$.[50] We will therefore keep its description short. There is exactly one independent position for each atom kind of TiNiSi. In the case of $ZrA_\delta Sb_{2-\delta}$, these are the Zr site, the Q1 site (mixed occupied by Si or Ge and Sb) and the Sb2 site, a pure Sb position. A projection onto the *a*,*c* plane is given in Figure 1.

The Zr atom is located in a tricapped trigonal prism, whose nine vertexes are occupied by four Q1 atoms and five Sb2 atoms. The Zr−Q1 bonds are significantly shorter than the Zr−Sb2 bonds; e.g. for $ZrGe_{0.21}Sb_{1.79}$, the Zr−Q1 bonds range from 292 to 305 pm and the Zr−Sb2 bonds from 302 to 320 pm (Table 3). The same trend is observed in the structure of $HfGe_{0.2}Sb_{1.8}$ but not in the isostructural binary phosphide ZrP_2. Also, the Zr−Q1 distances decrease with increasing Si content from $ZrSi_{0.06}Sb_{1.94}$ to $ZrSi_{0.11}Sb_{1.89}$.

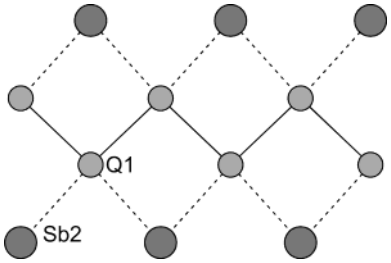

Figure 2. Anionic substructure of $ZrA_\delta Sb_{2-\delta}$ (horizontal: *b* axis).

For comparison it is noted that the Zr−Sb bonds in the true binary $ZrSb_2$ range from 294 to 303 pm and in ZrSb from 284 to 311 pm. The Zr−Si bonds in $ZrSi_2$ (starting at 268 pm)[51] and Zr−Ge bonds in $ZrGe_2$ (from 276 pm)[52] are significantly shorter than the corresponding Zr−Sb bonds, as expected on the basis of the differences in atomic radii (e.g., Slater radii:[53] $r_{Si} = 110$ pm; $r_{Ge} = 125$ pm; $r_{Sb} = 145$ pm). The unit cell volumes of $ZrSb_2$ and $ZrA_\delta Sb_{2-\delta}$ follow the same trend, from 0.2838(1) nm^3 for $ZrSi_{0.06}Sb_{1.94}$ to 0.28014(1) nm^3 for $ZrSi_{0.11}Sb_{1.89}$, with a cell volume of 0.57906 nm^3 for $ZrSb_2$ (normalized to four $ZrSb_2$ formula units as in $ZrA_\delta Sb_{2-\delta}$: 0.28953 nm^3).

A recent article[25] discussed the Sb atom substructures of (α-)$ZrSb_2$ and so-called "β-$ZrSb_2$" in detail. The structure of $ZrSb_2$ contains four crystallographically independent Sb sites that contribute to two distinct substructures. One is an Sb_2 pair, formed by the Sb4 atoms with an Sb−Sb distance of 307 pm. Such distances are often referred to as half bonds,[17,23,54,55] while single bonds are between 280 and 290 pm, as in the Zintl compound KSb (283−285 pm).[56] Viewing this bond as a half bond and assuming a full octet around each Sb atom, we assign a charge of −5 to the $Sb4_2$ dumbbell. The other three Sb atoms occur in an infinite Sb strip, with interatomic distances of 288, 309, and 310 pm that may be classified as single and half bonds, respectively. The Sb1 atom participates in one short single bond and two half bonds, Sb2 in four half bonds, and Sb3 in two half bonds. Applying the same counting scheme for Sb1−3, one obtains $(Zr^{3.25+})_2Sb1^-Sb2^-Sb3^{2-}Sb4^{2.5-}$.

On the other hand, there are only two atom sites for the A and Sb atoms in $ZrA_\delta Sb_{2-\delta}$: the Q1 site consisting of a mixture of Sb and up to 20% A (A = Si, Ge) and Sb2, a pure Sb site. These form one-dimensional strips; one thereof is shown in Figure 2 as marked in Figure 1. Each Q1 atom forms two short bonds to neighboring Q1 sites (284−289 pm) and two longer ones to Sb2 sites (311−315 pm), while the Sb2 atom participates only in two Sb2−Q1 bonds.

If we treat as above the short bond as a single bond and the longer one as a half bond, the Q1 site would be assigned five valence electrons and Sb2 seven (assuming the validity

(43) Cheng, J.; Franzen, H. F. *J. Solid State Chem.* **1996**, *121*, 362−371.
(44) Miller, G. J.; Cheng, J. *Inorg. Chem.* **1995**, *34*, 2962−2968.
(45) Kleinke, H.; Franzen, H. F. *J. Am. Chem. Soc.* **1997**, *119*, 12824−12830.
(46) Kleinke, H. *Trends Inorg. Chem.* **2001**, *7*, 135−149.
(47) Conrad, M.; Harbrecht, B. *Z. Anorg. Allg. Chem.* **1997**, *623*, 742−748.
(48) Kleinke, H. *Can. J. Chem.* **2001**, *79*, 1338−1343.
(49) Huber, M.; Deiseroth, H.-J. *Z. Kristallogr.* **1994**, *209*, 370.
(50) Trzebiatowski, W.; Weglowski, S.; Lukaszewicz, K. *Rocz. Chem.* **1958**, *32*, 189−201.
(51) Schachner, H.; Nowotny, H.; Kudielka, H. *Monatsh. Chem.* **1954**, *85*, 1140−1153.
(52) Smith, J. F.; Bailey, D. M. *Acta Crystallogr.* **1957**, *10*, 341−342.
(53) Slater, J. C. *J. Chem. Phys.* **1964**, *41*, 3199−3204.
(54) Bolloré, G.; Ferguson, M. J.; Hushagen, R. W.; Mar, A. *Chem. Mater.* **1995**, *7*, 2229−2231.
(55) Papoian, G. A.; Hoffmann, R. *Angew. Chem., Int. Ed.* **2000**, *39*, 2408−2448.
(56) Hönle, W.; von Schnering, H.-G. *Z. Kristallogr.* **1981**, *155*, 307−314.

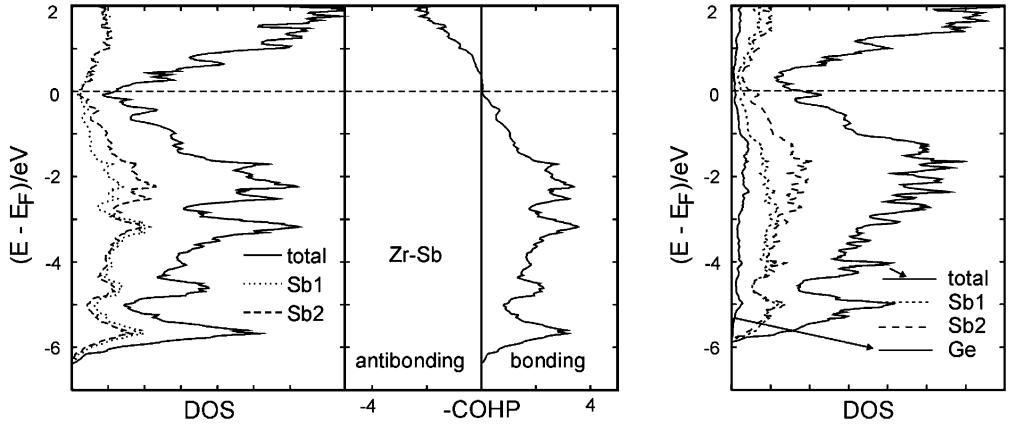

Figure 3. Left: Densities of states of "β-$ZrSb_2$". Middle: Zr−Sb COHP of "β-$ZrSb_2$". Right: Densities of states of "$ZrGe_{0.25}Sb_{1.75}$".

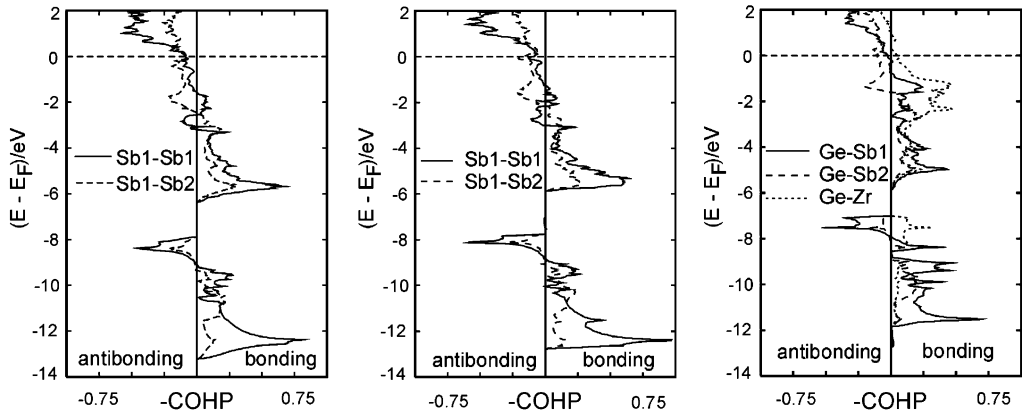

Figure 4. Left: Sb−Sb COHP's of "β-$ZrSb_2$". Middle: Sb−Sb COHP's of "$ZrGe_{0.25}Sb_{1.75}$". Right: COHP's with Ge of "$ZrGe_{0.25}Sb_{1.75}$".

of the octet rule). This leads to the formulation $Zr^{2+\delta+}(A^-)_\delta$-$(Sb1^0)_{1-\delta}Sb2^{2-}$. While this formalism can only be a crude approximation, it does readily explain why the tetrel atoms prefer the Q1 site over the Sb2 site, namely because of its fewer valence electrons. The same argument might be used to understand why replacing a few percent of the Sb atoms in $ZrSb_2$ leads to a structural change: all Sb atom sites in $ZrSb_2$ dispose of at least six valence electrons and may thus be less suited for a tetrel atom.

Electronic Structure. To illustrate the differences between hypothetical "β-$ZrSb_2$" and $ZrA_\delta Sb_{2-\delta}$, the corresponding densities of states of "β-$ZrSb_2$" and "$ZrGe_{0.25}Sb_{1.75}$", calculated with the LMTO method, are compared in Figure 3. A previous DOS calculation of "β-$ZrSb_2$" based on the extended Hückel approximation[57,58] gave comparable results.[24]

The DOS of "β-$ZrSb_2$" in the energy window shown (left part of Figure 3) comprises two peaks that overlap. At the bottom, starting below −6 eV, a large peak is dominated by Sb-p states; with some Zr contributions that come from covalent Zr−Sb mixing. This peak overlaps with the Zr-d peak so that a local nonzero minimum results directly at the Fermi level, pointing toward metallic properties. A comparison of Sb1 and Sb2 shows that Sb2 has more valence electrons, an observation that confirms in principle the above-mentioned counting scheme of five valence electrons for Sb1 and seven for Sb2.

Weighing the DOS into bonding and antibonding Zr−Sb states (crystal orbital Hamilton population, COHP,[59] curve, middle of Figure 3) shows a transition between bonding and antibonding character directly at the Fermi level. Thus, lowering (or raising) the valence-electron concentration by a partial replacement of Sb with Ge would result in overall weaker Zr−Sb bonding, if the electronic structure would remain unchanged. That the latter is true in a good approximation may be taken from comparing the DOS of "$ZrGe_{0.25}Sb_{1.75}$" (right part of Figure 3) with that of "β-$ZrSb_2$". The general peak shapes resemble each other closely from one DOS to the other, and the Fermi level of "$ZrGe_{0.25}$-$Sb_{1.75}$" is shifted into the Sb-dominated peak, down from the local nonzero minimum. Overall, the DOS of "$ZrGe_{0.25}$-$Sb_{1.75}$" is shifted up by about 0.4 eV, because the Fermi level was arbitrarily fixed at 0 eV in both DOS curves.

Additional differences, however, are present, which are more visible in comparing the different bonding interactions of the anionic substructures: the COHP curves of all different interactions with the Ge/Sb strip are shown in Figure 4, each of them averaged per bond. The left part displays the two different Sb−Sb interactions of "β-$ZrSb_2$". In both cases, the filled bonding states outweigh the bonding ones, while antibonding states are filled in the Sb-s as well as Sb-p

(57) Hoffmann, R. *J. Chem. Phys.* **1963**, *39*, 1397−1412.
(58) Whangbo, M.-H.; Hoffmann, R. *J. Am. Chem. Soc.* **1978**, *100*, 6093−6098.
(59) Dronskowski, R.; Blöchl, P. E. *J. Phys. Chem.* **1993**, *97*, 8617−8624.

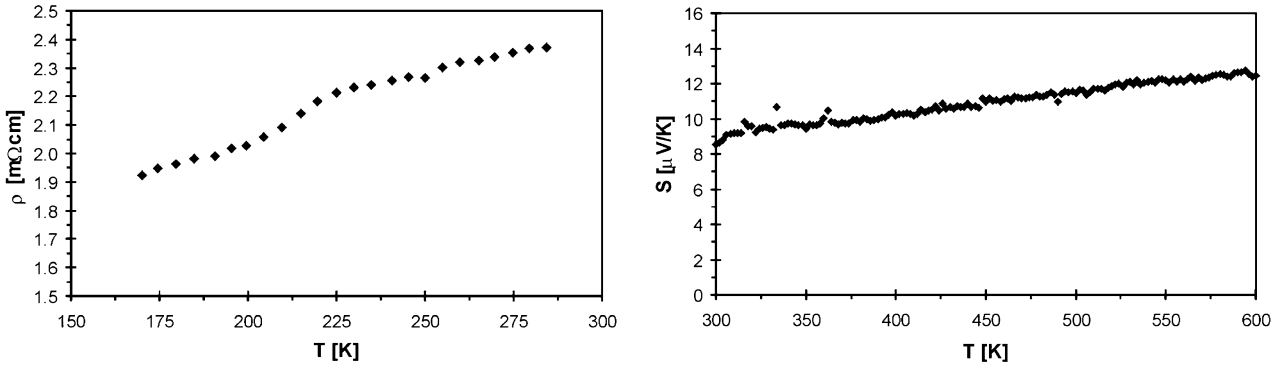

Figure 5. Specific resistivity (left) and Seebeck coefficients (right) of $ZrGe_{0.2}Sb_{1.8}$.

region. It is evident that the ratio is different; in the case of the shorter bond (solid line), the ratio of filled bonding to filled antibonding states is much higher. Since both interactions comprise antibonding states at the Fermi level, lowering the valence-electron concentration would depopulate the Sb−Sb antibonding states, thus strengthening the bonds.

This is notably different in the crystal orbital overlap population (COOP[60]) curves obtained via the extended Hückel calculations, where the Sb1−Sb1 interactions are basically nonbonding at the Fermi level (even slightly bonding).[24] A second difference between these COHP's and COOP's is that the Sb-s peak is completely bonding in the latter.

The Mulliken overlap population[61] for the short Sb1−Sb1 bonds of "β-$ZrSb_2$" of 0.43 electrons/bond is more than twice the MOP of the longer bond (0.17). That difference is even more distinct in our ICOHP calculations, which yielded −1.39 eV for the short and −0.45 eV for the longer bond, i.e., a ratio of 3:1. It is noted that ICOHP values typically have larger absolute values than MOP's[62,63] and of course always have different units; bonding character is reflected in negative ICOHP values.[64] Both the MOP's and ICOHP's confirm the above-mentioned counting of the short bond as a single (full) bond and the longer one as significantly bonding, while the ratio is not exactly 2:1 as expected for the ratio of single to half bonds.

The middle of Figure 4 clarifies how the Sb−Sb interactions change upon incorporation of Ge atoms into the Sb strip. While the main shapes remain virtually unchanged, integrating the curves up to the Fermi level yield almost 10% higher ICOHP values, namely −1.43 and −0.49, respectively, mainly because fewer antibonding states are filled due to the reduced number of valence electrons of "$ZrGe_{0.25}Sb_{1.75}$", compared to "β-$ZrSb_2$".

The Ge-containing bonds of "$ZrGe_{0.25}Sb_{1.75}$" (right part of Figure 4) are quite comparable to the ones with Sb1 of "β-$ZrSb_2$". Since Ge is (slightly) less electronegative than Sb, its major contributions are shifted toward higher energies, compared to the Sb contributions. E.g., its p-peak has its maximum around −2 eV, while the Sb-p peak is centered around −3 eV, as evident from the Zr−Ge and the Zr−Sb interactions. Besides these differences, the similarities are obvious. Furthermore, the ICOHP values of the Sb−Ge bonds, compared to the Sb−Sb bonds, are of the same order, e.g. −1.31 for Sb1−Ge and −0.49 for Sb2−Ge and −1.43 for Sb1−Sb1 and −0.49 for Sb2−Sb1. This might explain the possibility of mixing Ge and Sb atoms on one site, despite differences in atomic radii and valence electrons.

Physical Properties. To verify the prediction of metallic character made by the electronic structure calculations, the electrical resistivity and the Seebeck coefficient were measured on $ZrGe_{0.2}Sb_{1.8}$ (Figure 5). As expected for a metallic compound, the specific resistivity increases almost linear with increasing temperature. Its absolute value at room temperature of 2.4 mΩ cm is rather high for a metal, e.g. 60 times higher than that of elemental zirconium (0.04 mΩ cm). This might suggest a strong grain boundary effect, as a microcrystalline sample was used for the measurement.

Similarly, the small (positive) Seebeck coefficients (varying from 8.5 to 12.5 μV/K between 300 and 600 K) are in agreement with metallic properties. Elemental zirconium is also a p-type conductor with a Seebeck coefficient of +8.9 μV/K at 300 K.[65]

Conclusion

The new germanide−antimonides $ZrGe_{0.2}Sb_{1.8}$ and $HfGe_{0.2}Sb_{1.8}$ are isostructural with "β-$ZrSb_2$", which actually is not a binary Zr antimonide but a silicide−antimonide $ZrSi_\delta Sb_{2-\delta}$ with at least $0.066(7) \leq \delta \leq 0.115(3)$. Of the two anionic sites, one is a pure Sb site (Sb2) and the other (Q1) is mixed occupied by Ge and Sb (or Si and Sb). These ternary compounds are new members of the growing family of anionic DFSO compounds, for mixed Ge/Sb occupancies that differ from site to site are necessary for the formation of these structures.

Of particular interest is the nonclassical anionic substructure that consists of infinite Ge/Sb strips. To a first approximation, these strips may be described on the basis of single (full) Q1−Q1 bonds and half Q1−Sb2 bonds.

(60) Hughbanks, T.; Hoffmann, R. *J. Am. Chem. Soc.* **1983**, *105*, 3528−3537.
(61) Mulliken, R. S. *J. Chem. Phys.* **1955**, *23*, 2343−2346.
(62) Lee, C.-S.; Kleinke, H. *Eur. J. Inorg. Chem.* **2002**, 591−596.
(63) Lee, C.-S.; Safa-Sefat, A.; Greedan, J. E.; Kleinke, H. *Chem. Mater.* **2003**, *15*, 780−786.
(64) Landrum, G. A.; Dronskowski, R. *Angew. Chem., Int. Ed.* **2000**, *39*, 1560−1585.
(65) Vedernikow, M. V.; Dvunitkin, V. G.; Zhumagulov, A. *Fiz. Tverd. Tela* **1978**, *20*, 3302−3305.

Valence-electron counting under the assumption of the octet rule then yields five valence electrons for the Q1 site and seven for the Sb2 site. As Ge atoms comprise fewer valence electrons and are (slightly) less electronegative than Sb, they exclusively occupy the Q1 site and not the Sb2 site.

Electronic structure calculations of the hypothetical "β-$ZrSb_2$" and a Ge-containing model structure show that these compounds should be metallic, independent of the Ge (or Si) content. This was experimentally confirmed on $ZrGe_{0.2}Sb_{1.8}$. Strong Zr−Sb and Zr−Ge bonds are evident, and the structure gains additional stabilization from Sb−Sb and Sb−Ge interactions.

Acknowledgment. Financial support from the NSERC, CFI, OIT (Ontario Distinguished Researcher Award for H.K.), the Province of Ontario (Premier's Research Excellence Award for H.K.), and the Canada Research Chair program (CRC for H.K.) is appreciated.

Supporting Information Available: One X-ray crystallographic file in CIF format. This material is available free of charge via the Internet at http://pubs.acs.org.

IC0347440